

1 **High virulence does not necessarily impede viral adaptation to a**  
2 **new host: A case study using a plant RNA virus**

3

4 Anouk Willemsen<sup>1</sup>, Mark P. Zwart<sup>1,2</sup>, Santiago F. Elena<sup>1,3</sup>

5

6 <sup>1</sup>Instituto de Biología Molecular y Celular de Plantas (IBMCP), Consejo Superior de  
7 Investigaciones Científicas-Universidad Politécnica de Valencia, Campus UPV CPI 8E,  
8 Ingeniero Fausto Elio s/n, 46022 València, Spain.

9 <sup>2</sup>Institute of Theoretical Physics, University of Cologne, Zùlpicher StraÙe 77, 50937 Cologne,  
10 Germany.

11 <sup>3</sup>The Santa Fe Institute, 1399 Hyde Park Road, Santa Fe, NM 87501, USA.

12

13 E-mail addresses: [anwill@ibmcp.upv.es](mailto:anwill@ibmcp.upv.es) (AW), [mark.zwart@wur.nl](mailto:mark.zwart@wur.nl) (MPZ),  
14 [sfelena@ibmcp.upv.es](mailto:sfelena@ibmcp.upv.es) (SFE).

15

16 Corresponding author: AW ([anwill@ibmcp.upv.es](mailto:anwill@ibmcp.upv.es))

17

18

19

20

21

22

23

24

## 25 **Abstract**

26 **Background:** When between-host selection pressures predominate, theory suggests that high  
27 virulence could hinder between-host transmission of microparasites, and that virulence  
28 therefore will evolve to lower levels that optimize between-host transmission. Highly virulent  
29 microparasites could also curtail host development, thereby limiting both the host resources  
30 available to them and their own within-host effective population size. High virulence might  
31 therefore curtail the mutation supply rate and increase the strength with which genetic drift  
32 acts on microparasite populations, thereby limiting the potential to adapt to the host and  
33 ultimately perhaps the ability to evolve lower virulence. As a first exploration of this  
34 hypothesis, we evolved *Tobacco etch virus* carrying an eGFP fluorescent marker in two semi-  
35 permissive host species, *Nicotiana benthamiana* and *Datura stramonium*, for which it has a  
36 large difference in virulence. We compared the results to those previously obtained in the  
37 typical host, *Nicotiana tabacum*, where we have shown that carriage of *eGFP* has a high  
38 fitness cost and its loss serves as a real-time indicator of adaptation.

39 **Results:** After over half a year of evolution, we sequenced the genomes of the evolved  
40 lineages and measured their fitness. During the evolution experiment, marker loss leading to  
41 viable virus variants was only observed in one lineage of the host for which the virus has low  
42 virulence, *D. stramonium*. This result was consistent with the observation that there was a  
43 fitness cost of *eGFP* in this host, while surprisingly no fitness cost was observed in the host  
44 for which the virus has high virulence, *N. benthamiana*. Furthermore, in both hosts we  
45 observed few lineages with increases in viral fitness, and host-specific convergent evolution  
46 at the genomic level was only found in *N. benthamiana*.

47 **Conclusions:** The results of this study do not lend support to the hypothesis that high  
48 virulence impedes microparasites' evolution. Rather, they exemplify that jumps between host  
49 species can be game changers for evolutionary dynamics. When considering the evolution of

50 genome architecture, host species jumps might play a very important role, by allowing  
51 evolutionary intermediates to be competitive.

52

53 **Keywords:** Adaptation, Experimental evolution, Host-pathogen interactions, Virulence, Virus  
54 evolution, Genome architecture evolution

55

56

57

58

59

60

61

62

63

64

65

66

67

68

69

70

71

## 72 **Background**

73 From both applied and fundamental perspectives, virulence is a key phenotypic trait of  
74 microparasites. In medicine and agriculture, it is crucial to understand mechanistically how  
75 microparasites harm the host, in order to devise effective interventions. From a more  
76 fundamental perspective, evolutionary biologists have long been interested in understanding  
77 why many microparasites are highly virulent. It has been suggested that virulence reduces  
78 between-host transmission, and that selection would therefore act to maximize between-host  
79 transmission by reducing virulence [1, 2]. High virulence would signal maladaptation, for  
80 example following a host-species jump, and eventually be selected against. The ubiquity of  
81 microparasitic virulence and the fact that many apparently well-adapted microparasites have  
82 high virulence led to a more sophisticated framework: the hypothesis that there are tradeoffs  
83 between virulence and transmission [2–5]. This framework posits that high levels of  
84 replication could increase the probability of a microparasite being transferred to a new host,  
85 whilst also increasing the probability that the host would die quickly and the temporal  
86 window for transmission would be very brief. Under this more plausible framework,  
87 virulence evolves to the level that optimizes between-host transmission [4, 6, 7].

88 The tradeoff hypothesis forms the cornerstone for theoretical frameworks considering the  
89 evolution of virulence in many different pathosystems. Many important additions to the  
90 framework have been made, for example recognizing that within-host competition and  
91 opportunism can lead to increases in virulence [8–10]. Moreover, the importance of other  
92 factors at the between-host level have been given consideration, such as self-shading [11].  
93 Self-shading occurs when the host population is structured, and a highly virulent  
94 microparasite kills all host organisms in a subpopulation before transmission to another  
95 subpopulation can be achieved. The effects of evolution on microparasitic virulence have

96 therefore been given considerable attention, although the number of experimental studies that  
97 address this issue is still rather limited, especially for viruses [12].

98 The effects of evolution on microparasite virulence have been widely considered. However,  
99 virulence itself could also have profound effects on evolution, including its own evolutionary  
100 dynamics [13]. This reversed causality is already apparent from the tradeoff model, under  
101 which microparasites with suboptimal virulence will undergo reduced between-hosts  
102 transmission. All other things equal, if a smaller number of hosts are infected effective  
103 population size will be decreased, increasing the strength of genetic drift and decreasing the  
104 mutation supply rate. In addition, the evolution to optimum virulence may be slow as this  
105 optimum is not static and can shift towards lower virulence as the density of susceptible hosts  
106 decreases [14]. Moreover, a wide range of virulence can be associated with each step of  
107 evolution towards the optimum, where selection favors genotypes with higher fitness that may  
108 improve transmission but not necessarily improve virulence [13]. Besides these effects of  
109 virulence on evolution, it is conceivable that a similar within-host effect could also occur,  
110 when virulence curtails host development and thereby limits the host resources available to  
111 the microparasite. Virulence would then limit the microparasite effective population size  
112 within hosts, again reducing the mutation supply and thereby slowing the rate of adaptation.  
113 Interestingly, all of these mechanisms could limit the rate at which lower virulence evolves,  
114 meaning that high virulence might persist longer than suggested by the simple tradeoff model  
115 [13].

116 There are many reasons why high virulence in host-pathogen interactions could emerge, but  
117 the most likely avenue is probably a change of host species. For example, infection of Ebola  
118 virus in bats is asymptomatic, while in humans and other primates the death rate is high [15].  
119 Changes in virulence have been explained by the host phylogeny, where similar levels of  
120 virulence are displayed by closely related hosts and host jumps across large genetic distances

121 may result in high virulence [16]. However, if a microparasite is confronted with a new host  
122 environment in which its level of virulence is altered, how does virulence affect its ability to  
123 adapt to the new host?

124 Here we address this question using *Tobacco etch virus* (genus: *Potyvirus*, family:  
125 *Potyviridae*), a (+)ssRNA virus that infects a wide-range of host plants, and an experimental  
126 evolution approach. To consider the effect of virulence on virus adaptation, we looked for  
127 two natural host species in which (i) there was some evidence that TEV potential for  
128 adaptation would be roughly similar, and (ii) there was a large difference in virulence. The  
129 distribution of mutational fitness effects (DMFE) of TEV has been compared in eight host  
130 species, and this study concluded that there were strong virus genotype-by-host species  
131 interactions [17]. For many host species distantly related to the typical host of TEV,  
132 *Nicotiana tabacum*, the DMFE changed drastically; many mutations that were neutral or  
133 deleterious in *N. tabacum*, became beneficial. However, for two closely related host species,  
134 *Nicotiana benthamiana* and *Datura stramonium*, most mutations tested remained neutral or  
135 deleterious [17], implying that the fraction of beneficial mutations in both hosts is small.  
136 Moreover, virus accumulation after one week of infection is also similar for both hosts [18].  
137 On the other hand, TEV infection of *N. benthamiana* will typically result in heavy stunting  
138 and the death of the plant within a matter of weeks, whereas TEV infection of *D. stramonium*  
139 is virtually asymptomatic. Whilst there are many similarities between TEV infection in these  
140 two hosts, one key difference is host-pathogen interactions and therewith levels of viral  
141 virulence brought about.

142 As a first exploration of the effects of virulence on microparasite evolution, we therefore  
143 decided to evolve TEV in *N. benthamiana* and *D. stramonium*. By serially passaging each  
144 independent lineage in a single plant, our study maximizes within-host selection. This setup  
145 allows us to exclusively focus on effects of within-host selection, although for our model

146 system we expect to see large differences in the resulting population size and the scope of  
147 virus movement within the host. Moreover, to immediately gauge whether adaptive evolution  
148 might be occurring, we passaged a TEV variant expressing a marker protein (Fig. 1), the  
149 enhanced GFP (eGFP). Upon long-duration passages in *N. tabacum*, this exogenous sequence  
150 is quickly lost due to its strong fitness cost, and its loss is reliably indicated by a loss of eGFP  
151 fluorescence [19]. According to the above hypothesis that high virulence may impair the rate  
152 of microparasite evolution, we expect that adaptive evolution would occur more quickly in the  
153 host species for which TEV has lower virulence, *D. stramonium*, than in the host species for  
154 which it has high virulence, *N. benthamiana*. Hence, we expected that in *D. stramonium* (i)  
155 the eGFP marker would be lost more rapidly, (ii) there would be more sequence-level  
156 convergent evolution, and (iii) there would be larger increases in within-host competitive  
157 fitness. However, the results clashed with these simple hypotheses, exemplifying the extent  
158 to which a host species jump can be a game changer for RNA virus evolutionary dynamics.

159

## 160 **Methods**

### 161 **Virus stocks, plants and serial passages**

162 The TEV genome used to generate TEV-eGFP virus, was originally isolated from *N. tabacum*  
163 plants [20]. To generate a virus stock of the ancestral TEV-eGFP, the pMTEV-eGFP plasmid  
164 [21] was linearized by digestion with *Bgl*III prior to *in vitro* RNA synthesis using the  
165 mMESAGE mMACHINE<sup>®</sup> SP6 Transcription Kit (Ambion), as described in [22]. The third  
166 true leaf of 4-week-old *N. tabacum* L var Xanthi NN plants was mechanically inoculated with  
167 5 µg of transcribed RNA. All symptomatic tissue was collected 7 days post-inoculation (dpi).  
168 For the serial passage experiments, 500 mg homogenized stock tissue was ground into fine  
169 powder and diluted in 500 µl phosphate buffer (50 mM KH<sub>2</sub>PO<sub>4</sub>, pH 7.0, 3% polyethylene  
170 glycol 6000). From this mixture, 20 µl were then mechanically inoculated on the sixth true

171 leaf of 4-week old *N. benthamiana* Domin plants and on the third true leaf of 4-week old *D.*  
172 *stramonium* L plants. Ten independent replicates were used for each host plant. Based on a  
173 previous study done in *N. tabacum* [19], passages of TEV-eGFP in *D. stramonium* were done  
174 every 9 weeks. In *N. benthamiana* the virus induces host mortality, and therefore the  
175 passages had to be restricted to 6 weeks for this host. At the end of the designated passage  
176 duration all leaves above the inoculated one were collected and stored at  $-80^{\circ}\text{C}$ . For  
177 subsequent passages the frozen tissue was homogenized and a sample was ground and  
178 resuspended with an equal amount of phosphate buffer [19]. Then, new plants were  
179 mechanically inoculated as described above. Three passages were performed for lineages  
180 evolved in *D. stramonium* and five passages for lineages evolving in *N. benthamiana*, making  
181 the number of generations of evolution similar in both hosts. All plants were kept in a  
182 biosafety level 2 greenhouse at  $24^{\circ}\text{C}$  with 16 h light:8 h dark photoperiod.

183

#### 184 **Reverse transcription polymerase chain reaction (RT-PCR)**

185 To determine whether deletions occurred at the *eGFP* locus, RNA was extracted from 100 mg  
186 homogenized infected tissue using the InviTrap Spin Plant RNA Mini Kit (Strattec Molecular).  
187 Reverse transcription (RT) was performed using M-MuLV reverse transcriptase (Thermo  
188 Scientific) and reverse primer 5'-CGCACTACATAGGAGAATTAG-3' located in the 3'UTR  
189 of the TEV genome. PCR was then performed with Taq DNA polymerase (Roche) and  
190 primers flanking the *eGFP* gene: forward 5'-GCAATCAAGCATTCTACTTC-3', and reverse  
191 5'-CCTGATATGTTTCCTGATAAC-3'. PCR products were resolved by electrophoresis on  
192 1% agarose gels.

193

#### 194 **Virus accumulation and within-host competitive fitness assays**

195 Prior to performing assays, the genome equivalents per 100 mg of tissue of the ancestral virus  
196 stocks and all evolved lineages were determined for subsequent fitness assays. The InviTrap  
197 Spin Plant RNA Mini Kit (Strattec Molecular) was used to isolate total RNA of 100 mg  
198 homogenized infected tissue. Real-time quantitative RT-PCR (RT-qPCR) was performed  
199 using the One Step SYBR PrimeScript RT-PCR Kit II (Takara), in accordance with  
200 manufacturer instructions, in a StepOnePlus Real-Time PCR System (Applied Biosystems).  
201 Specific primers for the *CP* gene were used: forward 5'-TTGGTCTTGATGGCAACGTG-3'  
202 and reverse 5'-TGTGCCGTTTCAGTGTCTTCCT-3'. The StepOne Software v.2.2.2 (Applied  
203 Biosystems) was used to analyze the data. The concentration of genome equivalents per 100  
204 mg of tissue was then normalized to that of the sample with the lowest concentration, using  
205 phosphate buffer.

206 For the accumulation assays, 4-week-old *N. benthamiana* and *D. stramonium* plants were  
207 mechanically inoculated with 50 µl of the normalized dilutions of ground tissue. Inoculation  
208 of each viral lineage was done on the same host plant on which it had been evolved, plus TEV  
209 and the ancestral TEV-eGFP virus on each of the hosts, using three independent plant  
210 replicates per lineage. Leaf tissue was harvested 10 dpi. Total RNA was extracted from 100  
211 mg of homogenized tissue. Virus accumulation was then determined by means of RT-qPCR  
212 for the *CP* gene of the ancestral and the evolved lineages. For each of the harvested plants, at  
213 least three technical replicates were used for RT-qPCR.

214 To measure within-host competitive fitness, we used TEV carrying a red fluorescent protein:  
215 TEV-mCherry as a common competitor. This virus has a similar insert size and within-host  
216 fitness compared with TEV-eGFP [19]. All ancestral and evolved viral lineages were again  
217 normalized to the sample with the lowest concentration, and 1:1 mixtures of viral genome  
218 equivalents were made with TEV-mCherry [21]. The mixture was mechanically inoculated  
219 on the same host plant on which it had been evolved, plus TEV and the ancestral TEV-eGFP

220 virus on each of the hosts, using three independent plant replicates per viral lineage. The  
221 plant leaves were collected at 10 dpi, and stored at  $-80^{\circ}\text{C}$ . Total RNA was extracted from  
222 100 mg homogenized tissue. RT-qPCR for the *CP* gene was used to determine total viral  
223 accumulation, and independent RT-qPCR reactions were also performed for the mCherry  
224 sequence using specific primers: forward 5'-CGGCGAGTTCATCTACAAGG-3' and reverse  
225 5'-TGGTCTTCTTCTGCATTACGG-3'. The ratio of the evolved and ancestral lineages to  
226 TEV-mCherry ( $R$ ) is then  $R = (n_{CP} - n_{mCherry})/n_{mCherry}$ , where  $n_{CP}$  and  $n_{mCherry}$  are the  
227 RT-qPCR measured copy numbers of *CP* and *mCherry*, respectively. Then we can estimate  
228 the within-host competitive fitness as  $W = \sqrt[t]{R_t/R_0}$ , where  $R_0$  is the ratio at the start of the  
229 experiment and  $R_t$  the ratio after  $t$  days of competition [22]. The statistical analyses  
230 comparing the fitness between lineages were performed using R v.3.2.2 [23] and IBM SPSS  
231 Statistics version 23.

232

### 233 **Illumina sequencing, variants, and SNP calling**

234 For Illumina next-generation sequencing (NGS) of the evolved and ancestral lineages, the  
235 viral genomes were amplified by RT-PCR using AccuScript Hi-Fi (Agilent Technologies)  
236 reverse transcriptase and Phusion DNA polymerase (Thermo Scientific), with six independent  
237 replicates that were pooled. Each virus was amplified using three primer sets, generating  
238 three amplicons of similar size (set 1: 5'-GCAATCAAGCATTCTACTTCTATTGCAGC-3'  
239 and 5'-CCTGATATGTTTCCTGATAAC-3'; set 2: 5'-ACACGTACTGGCTGTCAGCG-3'  
240 and 5'-CATCAATGTCAATGGTTACAC-3'; set 3: 5'-CCCGTGAAACTCAAGATAG-3'  
241 and 5'-CGCACTACATAGGAGAATTAG-3'). Equimolar mixtures of the three PCR  
242 products were made. Sequencing was performed at GenoScreen (Lille, France:  
243 [www.genoscreen.com](http://www.genoscreen.com)). Illumina HiSeq2500  $2\times 100\text{bp}$  paired-end libraries with dual-index  
244 adaptors were prepared along with an internal PhiX control. Libraries were prepared using

245 the Nextera XT DNA Library Preparation Kit (Illumina Inc.). Sequencing quality control was  
246 performed by GenoScreen, based on PhiX error rate and Q30 values.  
247 Read artifact filtering and quality trimming (3' minimum Q28 and minimum read length of 50  
248 bp) was done using FASTX-Toolkit v.0.0.14 [24]. De-replication of the reads and 5' quality  
249 trimming requiring a minimum of Q28 was done using PRINSEQ-lite v.0.20.4 [25]. Reads  
250 containing undefined nucleotides (N) were discarded. Initially, the ancestral TEV-eGFP  
251 sequence was mapped using Bowtie v.2.2.6 [26] against the reference TEV-eGFP sequence  
252 (GenBank accession: KC918545). Error correction was done using Polisher v2.0.8 (available  
253 for academic use from the Joint Genome Institute) and a consensus sequences was defined for  
254 the ancestral TEV-eGFP lineage. Subsequently, the cleaned reads of the evolved sequences  
255 were mapped using Bowtie v.2.2.6 against the new defined consensus sequence. Single  
256 nucleotide mutations for each viral lineage were identified using SAMtools' mpileup [27] and  
257 VarScan v.2.3.9 [28], where the maximum coverage was set to 40000 and mutations with a  
258 frequency < 1% were discarded. Note that the single nucleotide mutations detected here can  
259 be fixed (frequency > 50%) in the evolved lineages, as the detection was done over the  
260 ancestral population. Hence, it allows us to compare the mutations that arose by evolving  
261 TEV-eGFP in the different hosts.

262

## 263 **Results**

### 264 **Experimental setup and fluorescent marker stability upon passaging of TEV-eGFP**

265 TEV-eGFP was mechanically passaged in *N. benthamiana* and *D. stramonium*. In a previous  
266 study we noted that 9-week long passages led to rapid deletion of *eGFP* as well as rapid  
267 convergent evolution in *N. tabacum* [19]. Although 9-week passages could be performed in  
268 *D. stramonium*, for *N. benthamiana* this was not possible due to virus-induced host mortality.  
269 These plants died after 6 weeks of infection, and therefore we were forced to collect tissue at

270 this time point. As *D. stramonium* grows to similar heights as *N. tabacum* when infected with  
271 TEV, and *N. benthamiana* does not grow much after infection, we chose to maximize  
272 infection duration to make the results comparable to those obtained in *N. tabacum* [19]. We  
273 performed three 9-week passages in *D. stramonium* and – to keep the total evolutionary time  
274 comparable – five 6-week passages in *N. benthamiana*. In *D. stramonium* all ten lineages  
275 initiated were completed, whereas in *N. benthamiana* only 6/10 lineages were completed.  
276 The remaining four *N. benthamiana* lineages failed to cause infection in subsequent rounds of  
277 passaging, and were therefore halted. Initial symptomatology of TEV-eGFP in *N.*  
278 *benthamiana* was very mild, while this symptomatology was more severe in the second and  
279 subsequent passages, possibly indicating adaptation of the virus to this alternative host. In *D.*  
280 *stramonium* the symptomatology was constant along the evolution experiment.

281 Based on previous results, we expected that the exogenous *eGFP* gene sequence would be  
282 rapidly purged [19, 29, 30], and as such would serve as a first indicator of the occurrence of  
283 TEV adaptation. However, the usefulness of fluorescence for determining the integrity of the  
284 *eGFP* marker was limited in both hosts, by (i) the high levels of autofluorescence in the  
285 highly symptomatic *N. benthamiana* leaves, and (ii) the patchy fluorescence in the *D.*  
286 *stramonium* tissue. Therefore, unlike for TEV-eGFP in *N. tabacum*, the fluorescent marker  
287 was of limited use here. Nevertheless, all *N. benthamiana* lineages appeared to have some  
288 fluorescence until the end of the evolution experiment, and we observed a loss of fluorescence  
289 in only 1/10 *D. stramonium* lineages in the third 9-week passage.

290 After each passage, RNA was extracted from the collected leaf tissue, and RT-PCR with  
291 primers flanking the *eGFP* insert was performed. This RT-PCR assay can therefore detect  
292 deletions in the *eGFP* gene, even when deletions extend well into the downstream HC-Pro  
293 cistron [19]. In general, the RT-PCR results confirmed the fluorescence microscopy results:  
294 A large deletion was detected only in the one *D. stramonium* lineage with a loss of

295 fluorescence (Fig. 2A; 9-weeks passage 2 L8). This deletion variant went to a high frequency  
296 in the subsequent passage (Fig. 2A; 9-weeks passage 3 L8). For *N. benthamiana* lineages, we  
297 did detect a low-frequency deletion in the *eGFP* cistron in one lineage (Fig. 2B; 6-weeks  
298 passage 4 and 5 L4), but this deletion is so large that this variant is most likely no longer  
299 capable of autonomous replication. The deletion size is around 1500 nt, which means that  
300 after deleting the entire *eGFP*, around 800 nt are deleted from HC-Pro, which has a size of  
301 1377 nt in total. This deletion extends well into the central region of HC-Pro, beyond the  
302 well-conserved FRNK box, which is essential for virus movement and RNA-silencing  
303 suppressor activity [31, 32]. We performed an extra round of passaging with all *N.*  
304 *benthamiana* lineages to check whether this variant would remain at a low frequency, and  
305 found exactly this result (Fig. 2B; 6-week passage 6 L4). Furthermore, we detected a small  
306 deletion in one lineage (Fig. 2B; 6-week passage 5 and 6 L1) that was maintained at a low  
307 frequency in subsequent passages of the virus population.

308

### 309 **Whole-genome sequencing of the evolved lineages**

310 All evolved and the ancestral TEV-eGFP lineages were fully sequenced by Illumina  
311 technology (SRA accession: SRP075180). The consensus sequence of the ancestral TEV-  
312 eGFP population was used as a reference for mapping the evolved lineages. The deletion  
313 observed by RT-PCR (Fig. 2A) in one of the *D. stramonium* lineages was confirmed by a low  
314 number of reads mapping inside the *eGFP* region (median coverage *eGFP*: 111.5), compared  
315 to a higher average coverage outside this region (median coverage *PI* gene: 19190, median  
316 overall genome coverage: 18460). The large deletion included the N-terminal region of *HC-*  
317 *Pro*, as observed for other deletions that occur after gene insertions before this gene [19, 34].  
318 For all other lineages in *D. stramonium* and *N. benthamiana*, coverage over the genome was

319 largely uniform and similar to the ancestral virus population, indicating that there were indeed  
320 no genomic deletions present at appreciable frequencies.

321 Single nucleotide mutations were detected from a frequency as low as 1%, comparing the  
322 evolved TEV-eGFP lineages in *N. benthamiana* and *D. stramonium* to the ancestral  
323 population (Fig. 3). This detection was also performed for evolved TEV-eGFP lineages in *N.*  
324 *tabacum*, that were sequenced in a previous study [19] (SRA accession: SRP075228). In the  
325 evolved *N. benthamiana* lineages 165 unique mutations were found, with a median of 34.5  
326 (range: 27 - 47) mutations per lineage. In the evolved *D. stramonium* lineages 239 unique  
327 mutations were found, with a median of 31.5 (range: 16 - 35) mutations per lineage. In the  
328 evolved *N. tabacum* lineages, 183 unique mutations were found, with a median of 21.5  
329 (range: 17 - 36) mutations per lineage. Note that the single nucleotide mutations detected  
330 here can be fixed (frequency > 50%) in the evolved lineages, as the detection was done over  
331 the ancestral population. Hence, it allows us to compare the mutations that arose by evolving  
332 TEV-eGFP in the different hosts.

333 We detected only one mutation (U6286C; CI/Y2096H) that is shared between all three hosts.  
334 However, this mutation was present at a low frequency and not detected in all *D. stramonium*  
335 and *N. tabacum* lineages (Fig. 3 and Table 1). The *N. benthamiana* and *D. stramonium*  
336 lineages share more mutations (15) than either *N. benthamiana* or *D. stramonium* share with  
337 *N. tabacum* (4 and 9, respectively). However, most of these mutations are present in only a  
338 few lineages and at low frequency (Fig. 3 and Table 1).

339 The synonymous mutations U7092C, A7479C and A8253C, that are shared between *D.*  
340 *stramonium* and *N. tabacum*, are present in the highest number of lineages and reach higher  
341 frequencies comparing all shared mutations detected in the three hosts. Despite of these  
342 mutations already being present in the ancestral population, the frequencies at which these  
343 mutations are present display interesting patterns. In both *D. stramonium* and *N. tabacum* the

344 mutations A7479C and A8253C are always detected at the same frequency within each  
345 lineage, suggesting a strong linkage between these mutations (Additional file 1: Fig. S1).  
346 Furthermore, the U7092C mutation never appears together with the former two mutations  
347 (Additional file 1: Fig. S1), suggesting that this mutation occurs in another haplotype and that  
348 there may be sign epistasis between these two combinations of synonymous mutations.  
349 Interestingly, the ancestral U7092C, A7479C and A8253C mutations were not detected in the  
350 *N. benthamiana* lineages, demonstrating the differences in host-pathogen interactions.  
351 Host-specific mutations were mostly found in the evolved TEV-eGFP lineages of *N.*  
352 *benthamiana* (Fig. 3 and Table 2). In this host, a total number of 7 specific mutations were  
353 detected, all of them being nonsynonymous. In *D. stramonium* no host-specific mutations  
354 were detected. And in *N. tabacum* only one host-specific mutation was detected in the 3'UTR  
355 (Table 2). Note that host specific mutations were defined as mutations detected in at least  
356 half of the evolved lineages. For more information on the mutations found in the three hosts  
357 please see Additional file 2: Tables S1-S3.

358

### 359 **Viral accumulation and within-host competitive fitness**

360 We measured virus accumulation 10 dpi, by RT-qPCR for a region within the coat protein  
361 gene (*CP*). In both host species, we found no statistically significant differences (*t*-test with  
362 Holm-Bonferroni correction) between TEV, TEV-eGFP and the lineages of TEV-eGFP  
363 evolved in that host (Fig. 4).

364 We then measured within-host competitive fitness by means of head-to-head competition  
365 experiments with TEV-mCherry, a virus with a different marker but similar fitness to TEV-  
366 eGFP [21]. Here we observed interesting differences between TEV and TEV-eGFP in the  
367 two different hosts. Whereas the TEV-eGFP had lower fitness than the wild-type virus in *D.*  
368 *stramonium* (Fig. 5, compare TEV and ancestral TEV-eGFP; *t*-test:  $t_4 = 13.438$ ,  $P < 0.001$ ),

369 there was no difference in *N. benthamiana* (Fig. 5, compare TEV and ancestral TEV-eGFP; *t*-  
370 test:  $t_4 = -1.389$ ,  $P = 0.237$ ). Our results therefore suggest that although there is a fitness cost  
371 associated with the *eGFP* cistron in *N. tabacum* [19] and *D. stramonium*, there is none in *N.*  
372 *benthamiana*. Interestingly, *N. tabacum* and *N. benthamiana* are more closely related to each  
373 other than either species is to *D. stramonium*, and yet the host species has a strong effect on  
374 the costs of a heterologous gene.

375 For the lineages evolved in *D. stramonium*, only for 1/10 lineages there was a significant  
376 increase in competitive fitness compared to the ancestral TEV-eGFP observed (Fig. 5, L8; *t*-  
377 test with Holm-Bonferroni correction:  $t_4 = -6.890$ ,  $P = 0.002$ ). This lineage is the only one to  
378 have a deletion in the *eGFP* insert. In *N. benthamiana*, 1/6 lineages had a significant increase  
379 in within-host fitness (Fig. 5, L4; *t*-test with Holm-Bonferroni correction:  $t_4 = -5.349$ ,  $P =$   
380 0.006). However, this increase in fitness probably is not associated with the large genomic  
381 deletion for three reasons: (i) the wild-type TEV without the *eGFP* cistron has a similar  
382 fitness compared to the ancestral TEV-eGFP, suggesting no deletions in *eGFP* would be  
383 beneficial, (ii) the RT-PCR results show that this variant occurs at a low frequency in the  
384 population, and therefore is unlikely to effect strongly the results of the competition assay,  
385 and (iii) this deletion variant remains at low frequency during the next round of passaging  
386 (Fig. 2B), suggesting that while frequency-dependent selection might occur, its fitness is not  
387 higher than the coevolving full-length TEV-eGFP. Moreover, another lineage of *N.*  
388 *benthamiana* where we did not detect any deletions, also appeared to have increased in fitness  
389 (Fig. 5, L6; *t*-test:  $t_4 = -4.0792$ ,  $P = 0.015$ ), however, after the Holm-Bonferroni correction  
390 not significantly. Interestingly, the lineage that did increase its fitness significantly (L4) is the  
391 only lineage that contains mutations in the 6K2 protein in this host (Additional file 2: Table  
392 S1). Therefore we speculate that single-nucleotide variation is one of the main driving forces  
393 for an increase in TEV-eGFP fitness in *N. benthamiana*.

394 These fitness measurements show that most lineages failed to adapt to the new host species.  
395 However, in the two cases that there were significant fitness increases, the underlying genetic  
396 changes were consistent with the expected route of adaptation. In *D. stramonium*, where  
397 *eGFP* has a high fitness cost, this sequence was deleted. In *N. benthamiana*, where *eGFP*  
398 apparently has not fitness cost, host-specific single-nucleotide variation was observed.

399

## 400 **Discussion**

401 We set out to explore the hypothesis that differences in virulence for different hosts could  
402 have an effect on the rate of virus adaptation in each host [13]. Although we find this  
403 hypothesis simple and provocative, the observed patterns in our experiments suggest that even  
404 in a controlled laboratory environment, reality will often be complex and hard to predict. We  
405 used a virus expressing an eGFP fluorescent marker in the hope that the loss of this marker  
406 could serve as a real-time indicator of adaptation. However, there were complications with  
407 this method, and a loss of fluorescence was only observed in a single *D. stramonium* lineage.  
408 RT-PCR and Illumina sequencing confirmed the loss of the eGFP marker in this case, and its  
409 integrity in all other lineages. The data of our competitive fitness assay demonstrate why the  
410 marker sequence was probably rather stable in *N. benthamiana*; *eGFP* does not appear to have  
411 a cost in this host species, in sharp contrast to the strong fitness cost observed in *D.*  
412 *stramonium* as well as previously observed in the more closely related host *N. tabacum* [19].  
413 We expect that the marker will eventually be lost, but only due to genetic drift and therefore  
414 at a slow rate.

415 What mechanisms might underlie the difference in the fitness costs of *eGFP* marker in these  
416 two host plants? In a previous study, we showed that the loss of the *eGFP* marker occurred  
417 more rapidly as the duration of each passage was increased [19]. During long passages  
418 transmission bottlenecks are more spaced on time, and much larger census population sizes

419 are reached. However, there is also much greater scope for virus movement into the newly  
420 developing host tissues. As for *N. tabacum* [19], here we again observed that the *eGFP*  
421 marker does not affect virus accumulation, whereas it does lower competitive fitness in *D.*  
422 *stramonium*. These observations suggest that the effects of the *eGFP* marker on virus  
423 movement are the main reason for selection against the marker. However, marker loss in *D.*  
424 *stramonium* appears to occur much slower compared to *N. tabacum* [19], indicating poor  
425 virus adaptation to this alternative host. Given the high virulence of TEV for *N. benthamiana*,  
426 including strong stunting, there will be limited virus movement during infection and thus  
427 significantly lower population census sizes. Hence, we speculate that in *N. benthamiana* the  
428 limited scope for virus movement and accumulation –due to the virus’ virulence itself– might  
429 mitigate the cost of the *eGFP* marker. Alternatively, cell-to-cell and systemic virus  
430 movement in *N. benthamiana* might be so slow that the addition of the *eGFP* marker matters  
431 little. A slow systemic virus movement may also explain why in the second round of  
432 infection four lineages failed to re-infect *N. benthamiana*, as initial virus accumulation  
433 appeared to be very low until possible virus adaptation by means of point mutations occurred.  
434 These results are at odds with our expectations, but they nevertheless have some interesting  
435 implications. First, host species changes can apparently ameliorate the costs of exogenous  
436 genes. Although strong virus genotype-by-host species interactions have been previously  
437 shown for TEV [17], we did not anticipate that a such a simple difference (the presence of  
438 *eGFP*) could also be subjected to such an interaction. These results suggest that when  
439 considering the evolution of genome architecture, host species might play a very important  
440 role, by allowing evolutionary intermediates to be competitive. For example, for TEV we  
441 have shown that the evolution of an alternative gene order through duplication of the *NiB*  
442 replicase gene is highly unlikely, as this intermediate step leads to significant decreases in  
443 fitness, making the trajectory to alternative gene orders inaccessible [34]. If *NiB* duplication

444 has a similar interaction with host species as the *eGFP* insert has, then an alternative host  
445 species could act as a stepping-stone and hereby increase the accessibility of the evolutionary  
446 trajectory to alternative gene orders. Similar effects of environmental change have been noted  
447 in other studies [35]. The generality of these results has not been addressed yet using other  
448 viruses with altered genome architecture, but the possibilities are tantalizing. Second, our  
449 results could also have implications for assessing the biosafety risks of the genetically  
450 modified organisms. Our results suggest that extrapolating fitness results from a permissive  
451 host to alternative hosts can be problematic, even when the scope for unexpected interactions  
452 appears to be limited, as would be the case for the addition of eGFP expression. In other  
453 model systems, unexpected interactions between heterologous genes and host species have  
454 also been reported [36].

455 Our results were not consistent with the hypothesis that high virulence could slow down the  
456 rate of adaptation, as in each host only a single lineage had evolved higher fitness. The low  
457 rate of adaptation observed was consistent with a previous report [18], although we used  
458 passages of a longer duration here and had therefore expected more rapid adaptation [19].  
459 Given the low rate at which lineages adapted in this experiment, however, we do not consider  
460 that our results provide strong evidence against the hypothesis. Nevertheless, our results do  
461 stress that differences in host biology can have a much stronger effect on evolutionary  
462 dynamics than differences in virus-induced virulence between host species. An alternative  
463 way to tackling the question of the effects of virulence on adaptation might be to use a  
464 biotechnological approach; hosts which have different levels of virulence can be engineered,  
465 to ensure the main difference between host treatment is microparasite-induced virulence. For  
466 example, plant hosts could be engineered to express antiviral siRNAs at low levels. Such an  
467 approach would allow for a more controlled test of the hypothesis suggested here, whilst  
468 probably not being representative for natural host populations. On the other hand, such

469 experiments could perhaps help shed light on the effects of virulence on adaptation in  
470 agroecosystems or vaccinated populations.

471

## 472 **Conclusions**

473 A host species jump can be a game changer for evolutionary dynamics. A non-functional  
474 exogenous sequence *-eGFP-* which is unstable in its typical host, has shown to be more  
475 stable in two alternative host species for which TEV has both lower and higher virulence than  
476 in the typical host. In addition, *eGFP* does not appear to have any fitness effects in the host  
477 for which TEV has high virulence. These observations clashed with the hypothesis that high  
478 virulence slows down the rate of adaptation. Moreover, when considering the evolution of  
479 genome architecture, host species jumps might play a very important role, by allowing  
480 evolutionary intermediates to be competitive.

481

## 482 **Declarations**

### 483 **Ethics approval and consent to participate**

484 Not applicable

485

### 486 **Consent for publication**

487 Not applicable

488

### 489 **Availability of data and material**

490 The raw read data from Illumina sequencing is available at SRA with accession: SRP075180.

491 The fitness data has been deposited on LabArchives with doi: 10.6070/H4N877TD.

492

### 493 **Competing interests**

494 The authors declare that they have no competing interests

495

## 496 **Funding**

497 This work was supported by the John Templeton Foundation [grant number 22371 to S.F.E];  
498 the European Commission 7<sup>th</sup> Framework Program EvoEvo Project [grant number ICT-  
499 610427 to S.F.E.]; and the Spanish Ministerio de Economía y Competitividad (MINECO)  
500 [grant numbers BFU2012-30805 and BFU2015-65037-P to S.F.E]. The opinions expressed in  
501 this publication are those of the authors and do not necessarily reflect the views of the John  
502 Templeton Foundation. The funders had no role in study design, data collection and analysis,  
503 decision to publish, or preparation of the manuscript.

504

## 505 **Author's contributions**

506 AW, MPZ and SFE designed the study. AW and MPZ performed the experiments. AW, MPZ  
507 and SFE analyzed the data and wrote the manuscript. All authors read and approved the final  
508 manuscript.

509

## 510 **Acknowledgements**

511 We thank Francisca de la Iglesia and Paula Agudo for excellent technical assistance.

512

## 513 **Additional files**

### 514 **Additional file 1:**

515 **Figure S1.** Frequency of mutations found in both *D. stramonium* and *N. tabacum*. Mutations  
516 detected in both *D. stramonium* and *N. tabacum* that were present in all the lineages of either  
517 one of these hosts. The frequency of these mutations in either the ancestral population (anc)

518 or the different lineages (L1-L10) is given by the color-coded points. The points are  
519 connected by the broken lines to emphasize the trend in the data.

520

521 **Additional file 2:**

522 **Table S1.** Mutations detected in the *Nicotiana benthamiana* lineages as compared to the  
523 ancestral lineage

524 **Table S2.** Mutations detected in the *Datura stramonium* lineages as compared to the  
525 ancestral lineage

526 **Table S3.** Mutations detected in the *Nicotiana tabacum* lineages as compared to the ancestral  
527 lineage

528

529 **References**

530 1. Ewald PW. Host-parasite relations, vectors, and the evolution of disease severity. *Annu*  
531 *Rev Ecol Syst.* 1983;14:465–485.

532 2. Alizon S, Hurford A, Mideo N, Van Baalen M. Virulence evolution and the trade-off  
533 hypothesis: history, current state of affairs and the future. *J Evol Biol.* 2009;22:245–259.

534 3. Fraser C, Hollingsworth TD, Chapman R, de Wolf F, Hanage WP. Variation in HIV-1 set-  
535 point viral load: Epidemiological analysis and an evolutionary hypothesis. *Proc Natl Acad Sci*  
536 *USA.* 2007;104:17441–17446.

537 4. de Roode JC, Yates AJ, Altizer S. Virulence-transmission trade-offs and population  
538 divergence in virulence in a naturally occurring butterfly parasite. *Proc Natl Acad Sci USA.*  
539 2008;105:7489–7494.

540 5. Mackinnon MJ, Gandon S, Read AF. Virulence evolution in response to vaccination: The  
541 case of malaria. *Vaccine.* 2008;26 Suppl 3:C42–C52.

542 6. Ebert D, Weisser WW. Optimal killing for obligate killers: the evolution of life histories

- 543 and virulence of semelparous parasites. *Proc R Soc B Biol Sci.* 1997;264:985–991.
- 544 7. Pagán I, Montes N, Milgroom MG, García-Arenal F. Vertical transmission selects for  
545 reduced virulence in a plant virus and for increased resistance in the host. *PLoS Pathog.*  
546 2014;10:e1004293.
- 547 8. May RM, Nowak MA. Coinfection and the evolution of parasite virulence. *Proc R Soc B*  
548 *Biol Sci.* 1995;261:209–215.
- 549 9. de Roode JC, Pansini R, Cheesman SJ, Helinski MEH, Huijben S, Wargo AR, Bell AS,  
550 Chan BHK, Walliker D, Read AF. Virulence and competitive ability in genetically diverse  
551 malaria infections. *Proc Natl Acad Sci.* 2005;102:7624–7628.
- 552 10. Brown SP, Cornforth DM, Mideo N. Evolution of virulence in opportunistic pathogens:  
553 generalism, plasticity, and control. *Trends Microbiol.* 2012;20:336–342.
- 554 11. Boots M, Sasaki A. The evolutionary dynamics of local infection and global reproduction  
555 in host-parasite interactions. *Ecol Lett.* 2000;3:181–185.
- 556 12. Bull JJ, Luring AS. Theory and Empiricism in Virulence Evolution. *PLoS Pathog.*  
557 2014;10:e1004387.
- 558 13. Bull JJ, Ebert D. Invasion thresholds and the evolution of nonequilibrium virulence. *Evol*  
559 *Appl.* 2008;1:172–182.
- 560 14. Lenski RE, May RM. The Evolution of Virulence in Parasites and Pathogens:  
561 Reconciliation Between Two Competing Hypotheses. *J Theor Biol.* 1994;169:253–265.
- 562 15. Leroy EM, Kumulungui B, Pourrut X, Rouquet P, Hassanin A, Yaba P, Délicat A,  
563 Paweska JT, Gonzalez J-P, Swanepoel R. Fruit bats as reservoirs of Ebola virus. *Nature.*  
564 2005;438:575–576.
- 565 16. Longdon B, Hadfield JD, Day JP, Smith SCL, McGonigle JE, Cogni R, Cao C, Jiggins  
566 FM. The Causes and Consequences of Changes in Virulence following Pathogen Host Shifts.  
567 *PLOS Pathog.* 2015;11:e1004728.

- 568 17. Lalić J, Cuevas JM, Elena SF. Effect of host species on the distribution of mutational  
569 fitness effects for an RNA virus. *PLoS Genet.* 2011;7:e1002378.
- 570 18. Bedhomme S, Lafforgue G, Elena SF. Multihost experimental evolution of a plant RNA  
571 virus reveals local adaptation and host-specific mutations. *Mol Biol Evol.* 2012;29:1481–  
572 1492.
- 573 19. Zwart MP, Willemsen A, Daròs JA, Elena SF. Experimental evolution of  
574 pseudogenization and gene loss in a plant RNA virus. *Mol Biol Evol.* 2014;31:121–134.
- 575 20. Carrington JC, Haldeman R, Dolja VV, Restrepo-Hartwig MA. Internal cleavage and  
576 trans-proteolytic activities of the VPg-proteinase (NIa) of tobacco etch potyvirus *in vivo*. *J*  
577 *Viro.* 1993;67:6995–7000.
- 578 21. Zwart MP, Daròs JA, Elena SF. One is enough: *in vivo* effective population size is dose-  
579 dependent for a plant RNA virus. *PLoS Pathog.* 2011;7:e1002122.
- 580 22. Carrasco P, Daròs JA, Agudelo-Romero P, Elena SF. A real-time RT-PCR assay for  
581 quantifying the fitness of *Tobacco etch virus* in competition experiments. *J Virol Methods.*  
582 2007;139:181–188.
- 583 23. R Core Team. R: A language and environment for statistical computing. 2014. Vienna,  
584 Austria: R Foundation for Statistical Computing. <http://www.R-project.org/>. Accessed 20  
585 June 2016.
- 586 24. FASTX-Toolkit. Hannon Lab. [http://hannonlab.cshl.edu/fastx\\_toolkit/index.html](http://hannonlab.cshl.edu/fastx_toolkit/index.html).  
587 Accessed 20 June 2016.
- 588 25. Schmieder R, Edwards R. Quality control and preprocessing of metagenomic datasets.  
589 *Bioinformatics.* 2011;27:863–864.
- 590 26. Langmead B, Salzberg SL. Fast gapped-read alignment with Bowtie 2. *Nat Methods.*  
591 2012;9:357–359.
- 592 27. Li H, Handsaker B, Wysoker A, Fennell T, Ruan J, Homer N, Marth G, Abecasis G,

- 593 Durbin R. The sequence alignment/map format and SAMtools. *Bioinformatics*.  
594 2009;25:2078–2079.
- 595 28. Koboldt DC, Zhang Q, Larson DE, Shen D, McLellan MD, Lin L, Miller CA, Mardis ER,  
596 Ding L, Wilson RK. VarScan 2: Somatic mutation and copy number alteration discovery in  
597 cancer by exome sequencing. *Genome Res*. 2012;22:568–576.
- 598 29. Dolja VV, Herndon KL, Pirone TP, Carrington JC. Spontaneous mutagenesis of a plant  
599 potyvirus genome after insertion of a foreign gene. *J Virol*. 1993;67:5968–5975.
- 600 30. Majer E, Daròs JA, Zwart M. Stability and fitness impact of the visually discernible  
601 Roseal marker in the *Tobacco etch virus* genome. *Viruses*. 2013;5:2153–2168.
- 602 31. Plisson C, Drucker M, Blanc S, German-Retana S, Le Gall O, Thomas D, Bron P.  
603 Structural characterization of HC-Pro, a plant virus multifunctional protein. *J Biol Chem*.  
604 2003;278:23753–23761.
- 605 32. Shibolet Y, Haronsky E, Leibman D, Arazi T, Wassenegger M, Whitham SA, Gaba V,  
606 Gal-On A. The conserved FRNK box in HC-Pro, a plant viral suppressor of gene silencing, is  
607 required for small RNA binding and mediates symptom development. *J Virol*.  
608 2007;81:13135–13148.
- 609 33. Verchot J, Carrington JC. Debilitation of plant potyvirus infectivity by P1 proteinase-  
610 inactivating mutations and restoration by second-site modifications. *J Virol*. 1995;69:1582–  
611 1590.
- 612 34. Willemsen A, Zwart MP, Tromas N, Majer E, Daros JA, Elena SF. Multiple Barriers to  
613 the Evolution of Alternative Gene Orders in a Positive-Strand RNA Virus. *Genetics*.  
614 2016;202:1503–1521.
- 615 35. de Vos MGJ, Dawid A, Sunderlikova V, Tans SJ. Breaking evolutionary constraint with a  
616 tradeoff ratchet. *Proc Natl Acad Sci USA*. 2015;112:14906–14911.
- 617 36. Hernández-Crespo P, Sait SM, Hails RS, Cory JS. Behavior of a recombinant baculovirus

618 in lepidopteran hosts with different susceptibilities. *Appl Environ Microbiol.* 2001;67:1140–

619 1146.

620

621 **Tables**622 **Table 1.** TEV-eGFP mutations shared in the different hosts

Nucleotide change	Amino acid change	Gene	<i>N. benthamiana</i>		<i>D. stramonium</i>		<i>N. tabacum</i>	
			Number of lineages	Frequency range	Number of lineages	Frequency range	Number of lineages	Frequency range
U6286C	Y2096H	CI	6/6	0.013 – 0.131	2/10	0.012 – 0.031	4/10	0.019 – 0.140
A208G	M70V	P1	1/6	0.012	1/10	0.010	-	-
C1039U	H347Y	P1	1/6	0.013	1/10	0.035	-	-
G1332A	M444I	eGFP	1/6	0.176	1/10	0.139	-	-
U1556G*	V519G	eGFP	1/6	0.011	6/10	0.010 – 0.016	-	-
U1836G	synonymous	HC-Pro	5/6	0.093 – 0.108	1/10	0.089	-	-
A1917G	synonymous	HC-Pro	1/6	0.015	1/10	0.017	-	-
A6278G	E2093G	CI	1/6	0.012	2/10	0.014 – 0.031	-	-
C6547U	H2183Y	VPg	1/6	0.013	1/10	0.014	-	-
U6747C	synonymous	VPg	1/6	0.012	1/10	0.110	-	-

A6776G	D2259G	VPg	2/6	0.533 – 0.746	1/10	0.023	-	-
G6803A	S2268N	VPg	1/6	0.014	1/10	0.024	-	-
A6438G	synonymous	6K2	1/6	0.012	1/10	0.024	-	-
C8405G*	T2802R	NIb	5/6	0.010 – 0.018	5/10	0.010 – 0.016	-	-
U9474C	synonymous	CP	1/6	0.013	1/10	0.061	-	-
C9837U	synonymous	CP	1/6	0.070	1/10	0.010	-	-
U3803C	I1268T	P3	2/6	0.656 – 0.881	-	-	2/10	0.010 – 0.019
U3872C	V2191A	P3	1/6	0.064	-	-	1/10	0.016
G4411A	V1471I	CI	1/6	0.030	-	-	1/10	0.016
C4989U	synonymous	CI	1/6	0.018	-	-	1/10	0.066
C548U	T183I	P1	-	-	1/10	0.011	1/10	0.024
G2928A*	synonymous	HC-Pro	-	-	1/10	0.017	1/10	0.999
U7092C*	synonymous	NIa-Pro	-	-	10/10	0.091 – 0.755	2/10	0.176 – 0.999
A7479C*	synonymous	NIa-Pro	-	-	10/10	0.132 – 0.790	7/10	0.960 – 0.999
A7567G	K2523E	NIa-Pro	-	-	4/10	0.012 – 0.053	10/10	0.015 – 0.871

G7710A	synonymous	NIa-Pro	-	-	1/10	0.014	1/10	0.024
A8253C*	synonymous	NIb	-	-	10/10	0.136 – 0.801	7/10	0.805 – 0.998
G9117A	synonymous	NIb	-	-	1/10	0.321	2/10	0.022 – 0.025
U9249C	synonymous	NIb	-	-	2/10	0.011 – 0.231	1/10	0.040

---

\*Also detected in the ancestral population

623 **Table 2.** Host specific mutations in the evolved TEV-eGFP lineages.

	<b>Nucleotide change</b>	<b>Amino acid change</b>	<b>Gene</b>	<b>Number of lineages</b>	<b>Frequency range</b>
<i>N. benthamiana</i>	G3797A	G1266E	P3	3/6	0.291 – 0.664
	G4380U	E1460D	6K1	3/6	0.012 – 0.093
	U4387C	Y1463H	6K1	4/6	0.011 – 0.016
	C4391U	T1464M	6K1	6/6	0.041 – 0.138
	G4397A	S1466N	CI	6/6	0.012 – 0.019
	A6771U	L2257F	VPg	4/6	0.027 – 0.201
	G8909U*	W2970L	NIb	5/6	0.026 – 0.042
<i>D. stramonium</i>	-	-	-	-	-
<i>N. tabacum</i>	G10253A		3'UTR	10/10	0.025 – 0.040

\*Also detected in the ancestral population.

624

## 625 **Figure Legends**

626 **Figure 1.** Schematic representation of TEV-eGFP. The *eGFP* gene is located between *PI*  
627 and *HC-Pro* cistrons. Proteolytic cleavage sites were provided at both ends of *eGFP*.

628

629 **Figure 2.** Deletion detection in the *eGFP* gene. Agarose gels with RT-PCR products of the  
630 region encompassing the *eGFP* gene. The TEV and TEV-eGFP are shown for comparative  
631 purposes. The negative controls are healthy plants and PCR controls (C-). (A) TEV-eGFP in  
632 *D. stramonium* has 10 independent lineages (L1-L10). A deletion encompassing the *eGFP*  
633 gene was detected in one lineage (L8) in the second 9-week passage. This deletion went to a  
634 high frequency in the subsequent passage. (B) TEV-eGFP in *N. benthamiana* has six  
635 independent lineages (L1-L6). A deletion bigger than the size of *eGFP* was detected in one  
636 lineage (L4) in the fourth 6-week passage. This deletion was not fixed in the two subsequent  
637 passages. A small deletion was detected in the fifth and sixth 6-week passage in L1.

638

639 **Figure 3.** Genomes of the TEV-eGFP lineages evolved the three different hosts as compared  
640 to the ancestral lineage. Mutations were detected using NGS data of the evolved lineages  
641 (L1-L10), as compared to their ancestral population. The square symbols represent mutations  
642 that are fixed (> 50%) and the circle symbols represent mutations that are not fixed (< 50%).  
643 Filled symbols represent nonsynonymous substitutions and open symbols represent  
644 synonymous substitutions. The triangle symbols represent mutations that are present in either  
645 the 3'UTR or 5'UTR. Black substitutions occur only in one lineage, whereas color-coded  
646 substitutions are repeated in two or more lineages. Note that the mutations are present at  
647 different frequencies as reported by VarScan 2. Grey boxes with continuous black lines  
648 indicate genomic deletions in the majority variant of the virus population. The grey  
649 transparent box with dotted black lines in L4 of *N. benthamiana* indicates a genomic deletion

650 in a minority variant. The latter box was drawn to indicate the size of the deletion, assuming  
651 that the deletion starts at the first position of *eGFP*. For more information on the frequency  
652 of the mutations please see Additional file 2: Tables S1-S3.

653

654 **Figure 4.** Virus accumulation of the evolved and ancestral lineages. Virus accumulation, as  
655 determined by accumulation experiments and RT-qPCR at 10 dpi, of TEV, the ancestral  
656 TEV-eGFP, and the evolved TEV-eGFP lineages in the corresponding hosts. TEV and the  
657 evolved lineage with a deletion in the *eGFP* gene are indicated with the orange bars. The  
658 ancestral TEV-eGFP and the evolved lineages with an intact *eGFP* gene are indicated with  
659 the green bars. Error bars represent SD of the plant replicates.

660

661 **Figure 5.** Within-host competitive fitness of the evolved and ancestral lineages. Fitness ( $W$ ),  
662 as determined by competition experiments and RT-qPCR of the different viral genotypes with  
663 respect to a common competitor; TEV-mCherry.  $W$  was determined at 10 dpi, of TEV, the  
664 ancestral TEV-eGFP, and the evolved TEV-eGFP lineages in the corresponding hosts. TEV  
665 and the evolved lineage with a deletion in the *eGFP* gene are indicated with the orange bars.  
666 The ancestral TEV-eGFP and the evolved lineages with an intact *eGFP* gene are indicated  
667 with the green bars. The orange asterisks indicate statistical significant differences of the  
668 evolved lineages as compared to TEV (*t*-test with Holm-Bonferroni correction). The green  
669 asterisks indicate statistical significant differences of the evolved lineages as compared to the  
670 ancestral TEV-eGFP (*t*-test with Holm-Bonferroni correction). Error bars represent SD of the  
671 plant replicates.

Figure 1

# TEV-eGFP

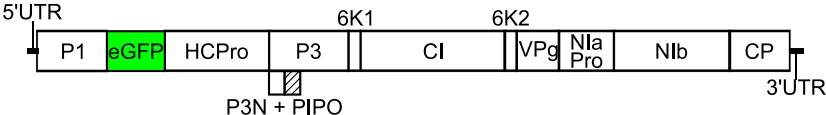
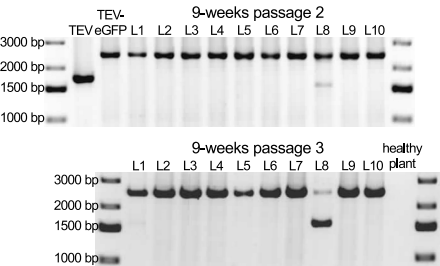


Figure 2

**A**

*Datura stramonium*



**B**

*Nicotiana benthamiana*

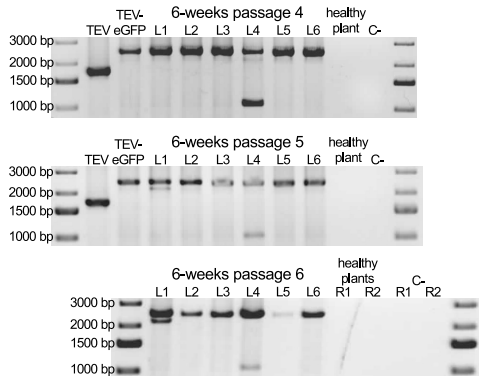


Figure 3

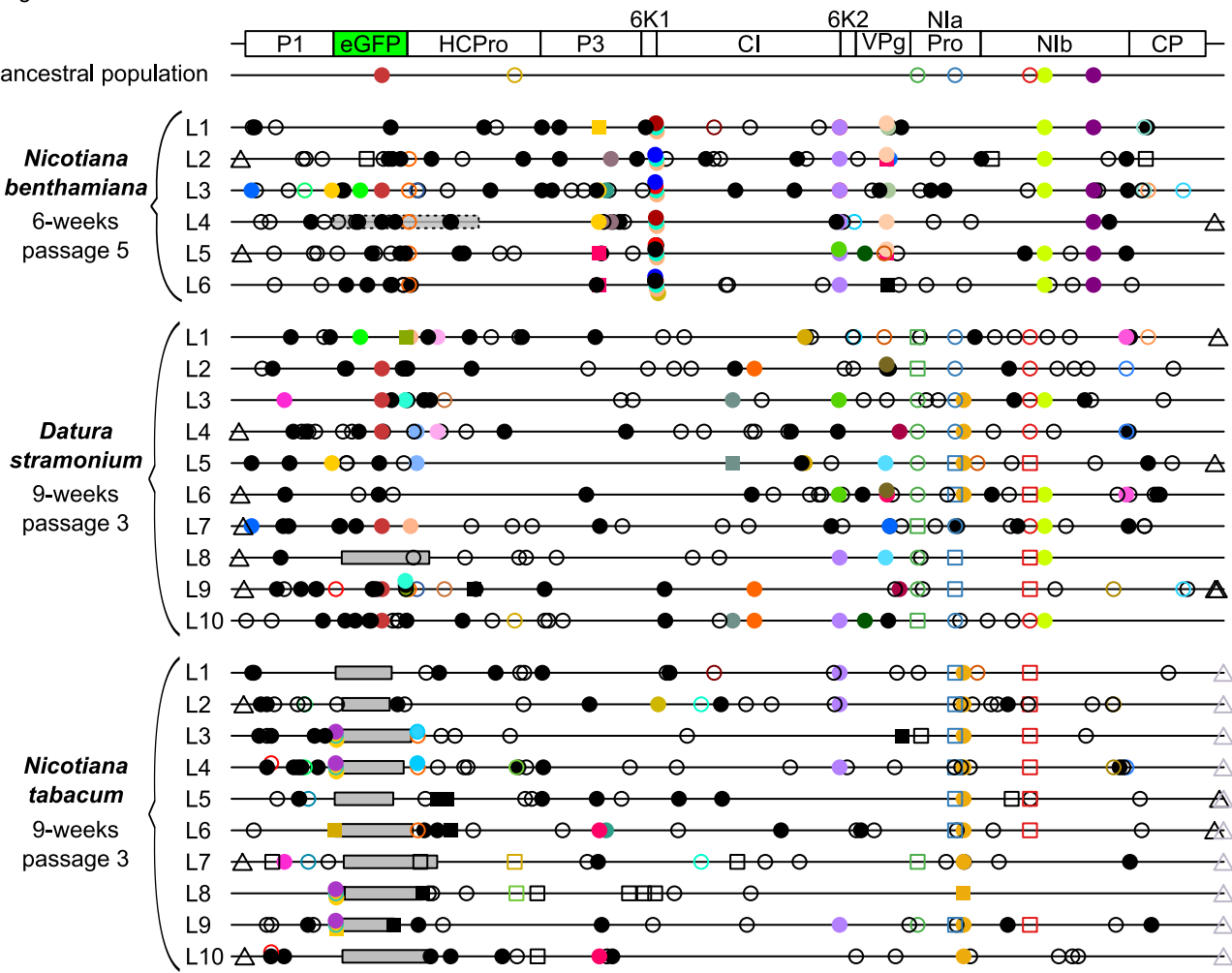


Figure 4

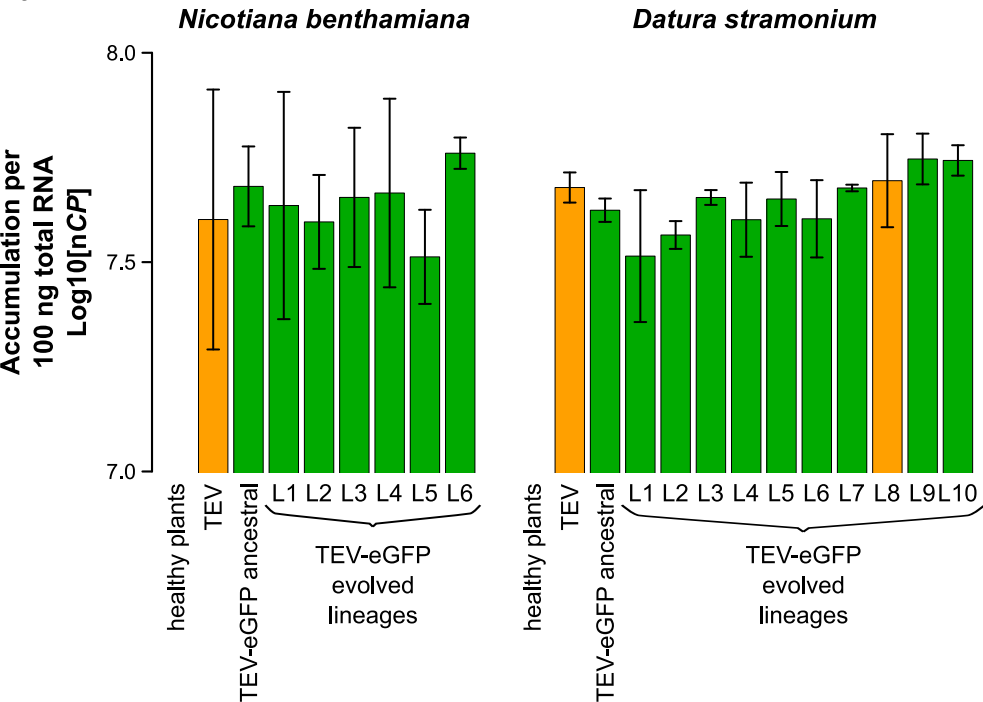


Figure 5

